The Structure and Decay Dynamics of Exciplexes Derived from Dibenzoylmethanatoboron Difluoride and Alkylbenzenes in Cyclohexane

Yuan L. Chow,*[a] Zhong-Li Liu,[b] C. Ingemer Johansson,[a] and Jun-ichi Ishiyama[a, c]

Abstract: Dibenzomethanatoboron difluoride ($DBMBF_2$) interacted with alkylbenzenes from its singlet excited state to form exciplexes ranging from weak polarity up to contact radical ion pairs (CRIP); this exciplex series shows the characteristics in the Marcus "normal" region. In cyclohexane these exciplexes gave intense fluorescence spectra and high quantum yields (Φ_{ex}^{∞}). The dipole moment of these exciplexes calculated from the solvatochromic shift of the fluorescence maximums (ν_{max}) was used to estimate the coefficient ("a" and "c") of the CT and LE terms in the exciplex wavefunction. On the basis of the measured lifetimes and Φ_{ex}^{∞} of these exciplexes, the radiative (k_f^{ex}) and nonradiative (k_{NR}^{ex}) rate constants were calculated. The former k_f^{ex} were also computed from a semi-empirical approach based on the assumption that the exciplex wavefunction could be adequately described by CT and LE states, and that $^*DBMBF_2$ primarily contributes to the probability of exciplex emission. Two results agree with each other with small systematic deviations for those less polar exciplexes. The plots of k_f^{ex} and k_{NR}^{ex} (or their logarithmic value) against the LE contribution (c^2) and transition energy gaps ($h\nu_{max}$) afford better correlation than those against $-\Delta G_{-et}$. This indicates the role played by the LE contribution in generating the stabilization energy (U_s) in these exciplexes through the $|A^-D^+\rangle \rightleftharpoons |^*AD\rangle$ resonance interaction; U_s, in turn, modifies $-\Delta G_{-et}$ to afford the decay driving force $h\nu_{max}$. Also, those plots from k_f^{ex} values (being determined directly from experiments) show better correlation than those from k_{NR}^{ex}. In contrast to the CRIP type exciplexes in the Marcus "inverted" region, these k_f^{ex} and k_{NR}^{ex} increase in the common trend with increasing transition energy gaps. The k_{NR}^{ex} plots show less steep slopes and attains more quickly a minimum toward the CRIP region; the latter is identified as the turning point from the "normal" to "inverted" region. Both the attenuation and reversal of the k_{NR}^{ex} value with increasing polarity are believed to be generated by the emerging contribution of the intersystem crossing process as an additional nonradiative process, which is induced by the increased spin–orbit coupling in highly polar exciplexes.

Keywords: electron transfer · exciplexes · fluorenscence · Marcus region · spin-orbit coupling

Introduction

The photochemical cycloaddition[1] and photoinduced cation radical reactions[2] occur concurrently from the interaction of a singlet excited 1,3-diketonatoboron difluoride with olefins or arenes. Generally the photocycloaddition of the BF_2 complexes is stereospecific and regioselective proceeding with high quantum efficiency.[1] These photoreactions are synthetically useful and offer a rare opportunity to investigate the mechanism of excited state behavior, particularly of the microscopic steps in which the excited state are partitioned in the two pathways.[3] This possibility is largely owing to the well defined singlet excited state properties and reactions exhibited by $DBMBF_2$ which has been used as the model BF_2 complex for investigation.[4] Much of the mechanistic information is undoubtedly stored in the electronic structure of the exciplexes formed between $^*DBMBF_2$ and substrates,[3] and may be gleaned from the kinetic and thermodynamic data of these exciplex decays.

Recently the Farid and co-workers[5] have, in a series of excellent publications, established the mechanism of return electron transfer reactions in the Marcus "inverted" region using CRIP (contact radical ion pairs) as an exciplex model; they took advantage of the fact that driving force differences and reorganization parameters for the reactions are common to the calculation of radiative as well as nonradiative rate constants.[6] Their conclusion that these rate constants become

[a] Prof. Y. L. Chow, Dr. C. I. Johansson, Prof. J.-i. Ishiyama
Department of Chemistry, Simon Fraser University
Burnaby, British Columbia, V5A 1S6 (Canada)
Fax: (604) 291-3765
E-mail: ychow@sfu.ca

[b] Prof. Z.-L. Liu
National Laboratory of Applied Organic Chemistry
Lanzhou University, Lanzhou, Gansu, 730000 (China)

[c] Prof. J.-i. Ishiyama
Visiting professor from Fukushima National College of Technology, Taira, Fukushima (Japan) in 1997.

  0947-6539/00/0616-2942 $ 17.50+.50/0

slower at higher exothermicity is a significant discovery in photoinduced electron transfer.[5, 6]

Our aim is to clarify the relation of the electronic energy level to the decay rate constants in this series of exciplexes, from which we hope to understand the pattern of driving forces behind these processes in the Marcus "normal" region. The theoretical basis of this study is the exciplex wavefunction which can be adequately described by Equation (1) as a two-state resonance hybrid as proposed previously.[3, 7]

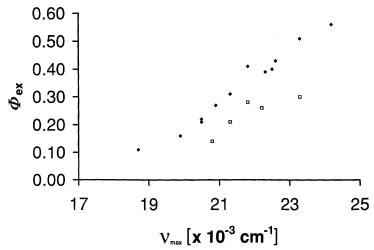

Figure 1. The plot of exciplex quantum yields Φ_{ex}^{∞} against the fluorescence maximums ν_{max} in cyclohexane; (□) represent exciplexes of *tert*-butylbenzenes.

Results

$DBMBF_2$ (A) interacts from its singlet excited state with a series of substituted benzenes as donors (D) to form highly fluorescent exciplexes in cyclohexane, though their fluorescence intensity is much reduced in polar solvent such as acetonitrile.[3b] For this study benzenes substituted with increasing number of methyl groups and those with at least one *tert*-butyl group were used as donors; quenching of $^*DBMBF_2$ fluorescence ($\Phi = 0.045$) by the donors was carried out in cyclohexane to ensure the formation of fluorescent exciplexes,[3b, 4] whose $h\nu_{max}$ were recorded in Table 1. The quantum yield of the exciplexes fluorescence in cyclohexane extrapolated to the total quenching of $^*DBMBF_2$ (Φ_{ex}^{∞}) was determined by the method and calculation described before.[3b] It is noteworthy that exciplex fluorescence derived from dialkyl or less substituted benzenes was extensively superimposed with the $^*DBMBF_2$ fluorescence band. For these cases the intensity for residual $DBMBF_2$ or exciplexes must be separated by a subtraction method.[3b] Repetitive measurements of some exciplex fluorescence derived from methyl substituted benzenes agreed well with those reported in the previous paper[3b] within experimental errors; those reported data were used as shown in Table 1. Φ_{ex}^{∞} was plotted against fluorescence peak energy (ν_{max}) to represent a decay driving force as shown in Figure 1, which is almost linear excluding those points of *tert*-butylbenzenes. A plot of Φ_{ex}^{∞} against the redox potential gap of the return electron trnasfer in these exciplexes (i.e., $-\Delta G_{-et} = E_{ox}^{D} - E_{red}^{A}$) gave much scatters, although those points with $-\Delta G_{-et} < 2.7$ eV (i.e., the exciplexes of higher than tetrasubstituted benzenes) were fairly linear.

The fluorescence maximum (ν_{max}) in a series of solvents was determined and plotted to afford the solvatochromic shifts correlation line. The slopes of these straight lines were used to calculate the "average" dipole moments (μ_{ex}) that were refined to the dipole moments (μ_{ex}^{0}) in vacuum. This refinement was not necessary for relatively large μ_{ex}, but was shown to be substantial for toluene and benzene (or those donors having similar E_{ox}^{D}). For the radical ion pair with complete one electron transfer, the CRIP μ_{ex}^{0} in this exciplex series was estimated to be 13.8 ± 0.5 eV (μ_{CRIP}^{0});[3b] for those with less than full one electron transfer, the CT% for each exciplexes was calculated according to Equation (1b), in which "a" and "c" are the coefficient of the exciplex wavefunction integrals.[3b] It was noted that there was an sharp CT% drop between the exciplexes of benzene and toluene. (see Table 1) owing to $E_{ox}^{D} \leq E_{ox}^{A}$ (= 2.45 eV).

$$\Psi_{ex} = a\,|A^{-}D^{+}\rangle + c\,|^*AD\rangle \qquad (1a)$$

Table 1. Radiative and radiationless rate constants and related properties of $DBMBF_2$/alkylbenzene exciplexes in cyclohexane.

	E_{ox} [eV]	$-\Delta G_{-et}$ [eV]	CT% [a^2]	ν_{max} [10^3 cm^{-1}]	Φ_{ex}^{∞}	k_f^{ex} [10^6 s^{-1}] obs.	calcd	$h\nu_{max}$ [eV]	k_{NR}^{ex} [10^6 s^{-1}] obs.
HMB	1.59	2.50	96 ± 4	18.7	0.11	4.3 ± 0.4	4 ± 4	2.32	35 ± 1
PMB	1.71	2.62	94 ± 2	19.9	0.16	6.6 ± 0.7	7 ± 5	2.46	34 ± 1
durene	1.79	2.70	91 ± 5	20.5	0.21	9.2 ± 0.9	12 ± 5	2.54	36 ± 1
1,2,3,5-TMB	1.83	2.73	90 ± 4	20.5	0.22	11 ± 1	13 ± 5	2.54	40 ± 1
1,2,3,4-TMB	1.82	2.74	88 ± 4	20.9	0.27	17 ± 2	15 ± 5	2.59	46 ± 2
1,2,4-TMB	1.92	2.83	83 ± 2	21.3	0.31	23 ± 2	23 ± 3	2.64	51 ± 2
mesitylene	2.02	2.93	73 ± 3	21.8	0.41	43 ± 6	39 ± 4	2.70	62 ± 12
p-xylene	2.06	2.97	80 ± 4	22.3	0.39	36 ± 5	32 ± 6	2.77	56 ± 10
m-xylene	2.14	3.05	76 ± 2	22.5	0.40	44 ± 6	40 ± 3	2.76	66 ± 12
o-xylene	2.13	3.04	74 ± 4	22.6	0.43	56 ± 8	43 ± 5	2.80	74 ± 13
toluene	2.25	3.16	51 ± 3	23.3	0.51	92 ± 13	59 ± 6	2.89	88 ± 24
benzene	2.62	3.53	21 ± 5	24.2	0.56	185 ± 30	150 ± 30	3.00	150 ± 45
tert-butylbenzene	2.21	3.12	62 ± 3	23.3	0.30	81 ± 12	65 ± 8	2.89	190 ± 18
4-*tert*-butyltoluene	2.06	2.97	76 ± 5	22.2	0.26	39 ± 6	14 ± 10	2.76	110 ± 10
5-*tert*-butyl-*m*-xylene	2.02	2.93	79 ± 4	21.8	0.28	35 ± 5	27 ± 3	2.20	91 ± 10
4-*tert*-butyl-o-xylene	1.92	2.83	89 ± 2	21.3	0.21	19 ± 2	13 ± 2	2.64	72 ± 2
5-*tert*-butyl-1,2,3-TMB	1.83	2.74	94 ± 2	20.8	0.14	10 ± 1	6 ± 3	2.58	62 ± 1

[a] The abbreviation of the substrates are hexamethylbenzene (HMB), pentamethylbenzene (PMB), 1,2,3,5-tetramethylbenzene (1,2,3,5-TMB), 1,2,4-trimethylbenzene (1,2,4-TMB). [b] The redox potential difference of the exciplex, $-\Delta G_{-et} = (E_{ox}^{D} - E_{red}^{A})$, was calculated from E_{ox}^{D} cited from previous publications[3a, b] and $E_{red}^{A} = -0.91$ eV. [c] The rate constants were calculated from Equation (2) where $(\tau_{ex})^{-1}$ was cited from the reference.[3c] [d] This is the modified figure on the basis of the experimental k_f^{ex} as discussed in the text; the unmodified value is $a^2 = 89 \pm 5$.

  0947-6539/00/0616-2943 $ 17.50+.50/0

$$a^2 = \mu_{ex}/\mu_{CRIP} \text{ and } a^2+c^2 \cong 1 \quad (1b)$$

$$k_f^{ex} = (\Phi_{ex}^{\infty})/\tau_{ex} \text{ and } (\tau_{ex})^{-1} - k_f^{ex} = k_{NR}^{ex} \quad (2)$$

Previously, we have measured the lifetime of these exciplexes using a time resolved fluorescence decay analysis in which the observed rate constant was defined[3c] as $(\tau_{obs})^{-1} = k_{-ex} + (\tau_{ex})^{-1}$. In the absence of the exciplex dissociation rate constant (i.e., k_{-ex} is negligible), $(\tau_{obs})^{-1} = (\tau_{ex})^{-1}$. In the present case $(\tau_{ex})^{-1} = k_f^{ex} + k_{NR}^{ex}$ where the latter two are the radiative and nonradiative rate constants (Scheme 1). Equation (2) showed the relation of the quantum yield of the exciplexes (Φ_{ex}^{∞}) to the radiative and nonradiative rate constants (k_f^{ex} and k_{NR}^{ex})[8] that are calculated and listed as the experimental rate constants in Table 1.

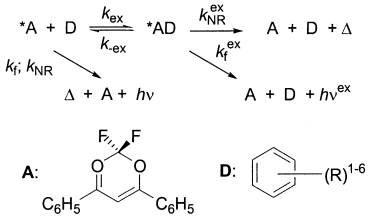

Scheme 1. Acceptor–donor complexes.

The radiative rate constant of exciplexes can be theoretically related to the transition dipole moment $\langle e\mathbf{r}\rangle$ connecting the excited and ground states,[7c, d] the transition of which is fully allowed for these exciplexes. The matrix element may be approximated so that the rate constant k_f^{ex} can be evaluated readily from experimental data. Firstly, the emission transition moment is given by the exciplex coupling integrals, in which charge transfer $\langle A^-D^+|\Sigma e\mathbf{r}|AD\rangle$ is neglected as has been shown by Mulliken[9] to be small. Secondly the locally excited term $\langle *AD|\Sigma e\mathbf{r}|AD\rangle$ is approximated[10] by $\langle *A|\Sigma e\mathbf{r}|A\rangle$ which can be accessed by *DBMBF$_2$ fluorescence data; this is based on the concept that radiative probability of exciplexes is mainly derived from that of a partner.[11] This led to an approximation of k_f^{ex} by Equation (3). Likewise the

$$k_f^{ex} \cong (64\pi^4/3hc^3)\, n^3 \nu_{max}^3\, c^2\, |\langle *A|\Sigma e\mathbf{r}|A\rangle|^2 \quad (3)$$

radiative rate constant for singlet excited DBMBF2 (k_f^A) can be cast into a similar form as in Equation (4). These two equations relate k_f^{ex} with k_f^A by Equation (5) through the

$$k_f^A = (64\pi^4/3hc^3)\, n^3 \nu_{ave}^3\, |\langle *A|\Sigma e\mathbf{r}|A\rangle|^2 \quad (4)$$

where $\nu_{ave} = 24\,200\ cm^{-1}$

$$k_f^{ex} \cong c^2\,(\nu_{max}/\nu_{ave})\, k_f^A \quad (5)$$

assumptions as stated above. Using the c values calculated from Equation (1b) and the experimental value[4] $k_f^A = \Phi_A/\tau_A$ $(= 0.045/0.23\ ns) = 2.0 \times 10^8\ s^{-1}$, k_f^{ex} was calculated from Equation (5) and listed in Table 1.

A plot of observed k_f^{ex} against the corresponding calculated values gave a good correlation line (Figure 2) except the point represented by the *p-tert*-butyltoluene/DBMBF2 exciplex

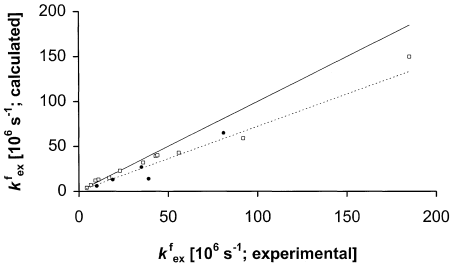

Figure 2. The plot of calculated k_f^{ex} against the experimental values in cyclohexane; (□) represent exciplexes of *tert*-butylbenzenes.

which showed abnormally low calculated k_f^{ex} values. As experimental data for ν_{max} and lifetime τ_{ex} for this exciplex[3b, c] did not show any anomaly from the general trends, the observed k_f^{ex} was adapted as "a better" value to estimate other parameters by backtracking in Equation (5). This retro-calculation gave $c^2 = 0.24$ and dipole moment of 10.5 debye unit (Table 1). The calculated k_f^{ex} values start to fall below the unit slope in Figure 2 beyond $k_f^{ex} > 35 \times 10^6\ s^{-1}$, that is those exciplexes from xylenes and below. The deviation may indicate the limit and extent of the validity of the assumptions made to derive Equations (3–5). Alternatively, it may hint the change of molecular shape causing solvent refractive index modification.[12] We noted that the point of deviation coincides with the onset of a contribution of stabilization energy (U_s) from the $|A^-D^+\rangle \rightleftharpoons |*AD\rangle$ resonance interaction as shown in the plot of ν_{max} in cyclohexane against $-\Delta G_{-et}$ $(= E_{ox}^D - E_{red}^A)$ (see Figure 4 in ref. [3b]).

Equation (5) predicted a linear correlation of k_f^{ex} versus c^2; such a plot using the observed k_f^{ex} was indeed reasonably straight with some scatters at least down to $c^2 \cong 0.1$ (Figure 3).

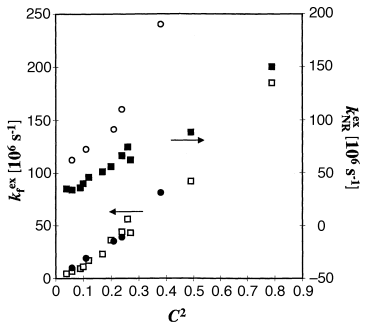

Figure 3. The plot of exciplex decay rate constants, k_f^{ex} and k_{NR}^{ex}, against c^2; (○) and (●) represent exciplexes of *tert*-butylbenzenes.

For comparison, k_{NR}^{ex} data were also plotted in Figure 3 showing two distinguishably independent correlation lines, one for those points derived from *tert*-butyl substituted benzenes and the other for those from methyl-substituted benzenes; both of them showed some scatters and significant curvature. The correlation of these two rate constants with CT% (or a^2) also gave a similar pattern with more curvature and scatters. In view of successful correlation of the radiative and nonradiative ($\log k_{-et}$) rate constants with the potential difference of return electron transfer $-\Delta G_{-et}$ for CRIP type exciplexes in the Marcus[5, 6] "inverted" region, similar plots were made of $\log k_f^{ex}$ and $\log k_{NR}^{ex}$ from Table 1 (Figure 4). Note

0947-6539/00/0616-2944 $ 17.50+.50/0 Chem. Eur. J. 2000, 6, No. 16

that nonradiative electron transfer k_{-et} (vide infra) represents all nonradiative processes[5a, 6c] and conceptually corresponds to our k_{NR}^{ex}.

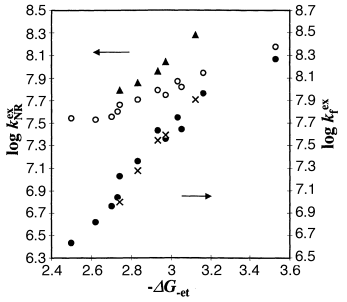

Figure 4. The plot of $\log k_f^{ex}$ and $\log k_{NR}^{ex}$ against the redox potential difference $-\Delta G_{-et} = (E_{ox}^{D} - E_{red}^{A})$ of exciplexes; (▲) and (×) represent exciplexes of *tert*-butylbenzenes.

The plots against $-\Delta G_{-et}$ in Figure 4 showed anything but improvement over the corresponding plots in Figure 3. While the $\log k_f^{ex}$ plot maintained reasonable linearity for whole range, the other $\log k_{NR}^{ex}$ plot showed more scatters and curbing. As in the present series the energy represented by exciplex fluorescence maximums more realistically express the stability (or the transition energy gap) of exciplexes, the correlation of $h\nu_{max}$ with $\log k_f^{ex}$ and $\log k_{NR}^{ex}$ was shown in Figure 5; indeed better linearity of points for both was obtained.

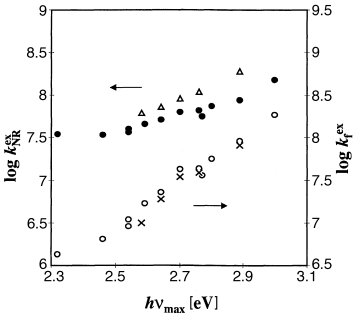

Figure 5. The plot of $\log k_f^{ex}$ and $\log k_{NR}^{ex}$ against the transition energy gap ($h\nu_{max}$); (△) and (×) represent exciplexes of *tert*-butylbenzenes.

Discussion

On quenching rate constants and exciplex electronic structures, the previous studies[3] have demonstrated that the present exciplex series of *DBMBF$_2$/benzenes behaves in the Marcus "normal" region. On the other hand, Farid's group[5] has studied a series of exciplexes in the Marcus "inverted" region, wherein CRIP-type exciplexes undergo radiative and nonradiative decays that are induced by the return electron transfer reaction. They were able to measure the rate constant of return electron transfer (k_{-et}) which was equated to the rate constant of nonradiative processes (vide supra). In contrast the present exciplex series possesses the CT contribution ranging from 20 to near 100%, namely a wide range of LE contributions, that is a theoretical basis for assigning this series in the Marcus "normal" region.[5] It is noted that the exciplexes derived from benzenes carrying a *tert*-butyl group behave at times independently and at others in consonance with those derived from methyl substituted benzenes. As the pattern is complex, their characteristics will be discussed together with other relevant phenomena as steric effects in a separate paper later.

In the present study, the interaction of singlet excited *DBMBF$_2$ with alkylbenzenes and subsequent exciplex formation have been studied in cyclohexane wherein the approach of substrates terminates at the exciplex stage regardless of electron transfer en route: This ensures the efficient formation of exciplexes and strong fluorescence therefrom.[3a] The major target of the investigation aims to clarify the driving force, among other factors, for the exciplex decay reactions. In studying a series of CRIP type exciplexes, it has been established that the return electron transfer induced k_f^{ex} and k_{NR}^{ex} share a common set of reorganization parameters and the rate constants are determined by the exothermicity of the CRIP in the form of $-\Delta G_{-et}$ and fluorescence maximums ν_{max}, both arising from RIP annihilation processes.[ab] The present exciplex series has a wide CT% ranging 20–100%, and shows various degrees of refinement in correlation depending on the type of parameters as shown in Figure 3, Figure 4 and Figure 5. Further, the plots show a strong quantitative relationship between k_f^{ex} and k_{NR}^{ex} as demonstrated by the common trend of the two plots. Both plots, however, increase as the oxidation potential E_{ox}^{D} increases (i.e., as $-\Delta G_{-et}$ or $h\nu_{max}$ increases), that is expected for the series being in the Marcus "normal" region. The extrapolation of plots in Figure 3 toward the CRIP state (i.e., $c^2 < 0.1$) shows that both k_f^{ex} and k_{NR}^{ex} are asymptotically approaching the limit near $10^6\ s^{-1}$ and $10^7\ s^{-1}$, respectively. These trends exist no matter the type of correlation parameters, though the correlation in Figure 5 (versus $h\nu_{max}$) is smoother in comparison to those in Figures 3 and 4 (versus c^2 and $-\Delta G_{-et}$). In all three Figures, generally the k_{NR}^{ex} plot is shallower, has more scatters and deviates from linearity faster than the k_f^{ex} plot; this will be discussed later. As k_{NR}^{ex} has been determined as the difference of the total exciplex decay and the radiative rate constants by Equation (2), it must contain other rate processes that do not emit. Being a composite term, k_{NR}^{ex} must contain compounded deviation originating from related experimental errors; this is a likely source of observed scatters.

The better correlation of k_f^{ex} and k_{NR}^{ex} in Figure 5 than in Figure 4 is a good indication that $-\Delta G_{-et}$ $(= E_{ox}^{D} - E_{red}^{A})$ calculated from the electrochemical data is a poor substitute for the exothermicity of the decay processes and not the sole source of the driving force for the transitions in this exciplex series. The use of $-\Delta G_{-et}$ to substitute for the exothermicity in CRIP type exciplexes is reasonably justifiable in the "inverted region" and has been successfully used in the computation and correlation of these rate constants induced by return electron transfer.[5, 6] For the present series in the Marcus "normal" region, the correlation with fluorescence energy $h\nu_{max}$ proved to give better results as shown by Figure 5 in comparison to Figure 4. As $h\nu_{max}$ is refined from $-\Delta G_{-et}$ by the stabilization energy U_s arising from the $|A^-D^+\rangle \rightleftharpoons |{}^*AD\rangle$ resonance interaction,[3a, b] a comparison of two Figures

emphasizes the importance of the LE contribution to the exciplex wavefunction (i.e., electronic configuration), and further, the role played by the resonance stabilization to quantitatively predict the driving force of exciplex decays.

As absorption and emission spectra can be recorded reasonably accurately, the radiative process and its rate constant are more studied parameters. The similar trends of the k_f^{ex} and k_{NR}^{ex} plots in Figure 3, Figure 4, and Figure 5 provide some insights that are summarized as below. Firstly, the common decreasing pattern of the both plots are good indications that the driving force and reorganization parameters for two processes share common characteristics. Secondly, both rate constants decrease with decreasing transition energy gaps (i.e., $h\nu_{max}$), that are different from the pattern in the Marcus "inverted region" and in agreement with that in the "normal region". Thirdly, a better correlation for k_f^{ex} values in these Figures undoubtedly shows that the reasonableness of experimental and calculated values by Equations (3–5); it justifies the use of the LE contribution c^2 to regulate the contribution of the transition dipole moment $\langle e\mathbf{r}\rangle$ accompanying the exciplex decay. Finally, the plots in Figures 3 and 5 share the common trend of converging on the far end; that demonstrates that both variables c^2 and $h\nu_{max}$ are closely related proportional parameters. In view that two parameters are indirectly connected through the exciplex dipole moment and wavefunction [as in Eq. (1)], the close resemblance in Figures 3 and 5 is a good statement on the validity of these calculations.[3b]

We wish to explore the nature of nonradiative processes involved in the k_{NR}^{ex} term, which generally shows poorer correlation than the k_f^{ex} term does. Exciplexes in the nonpolar end contain the LE contribution up to $c^2 = 0.8$ (see Figure 3); from this region k_{NR}^{ex} nearly proportionally decreases as c^2 shifts to below 0.2. The other extreme end is polar (or CRIP) exciplexes with $a^2 > 0.9$. It has been shown that moderately to weakly polar exciplexes posses strong internal conversions which dominate the nonradiative process.[13] This is arrived at on the basis of Equation (6) in which

$$k_{NR}^{ex} \text{ by intersystem crossing} \propto \langle {}^1{*}AD\,|\,H_{SO}\,|\,{}^3{*}AD\rangle + \langle A^-D^+\,|\,H_{SO}\,|\,{}^3{*}AD\rangle \quad (6)$$

the probability of intersystem crossing in this region is negligible since the coupling integral for the LE (first) term is insignificant, owing to the lack of spin–orbit couplings, in comparison to that of the CT (second) term.[13, 14] These conclusions are supported by the strong deuterium isotope effects that do operate during internal conversion, but not during intersystem crossing process.[13a] In agreement, we have shown that for those *$DBMBF_2$ exciplexes derived from xylenes or lower members the quantum yield of intersystem crossing is just about the same with that of the parent *$DBMBF_2$ and a minor process ($< 10\%$).[2c] Thus, an alternative contribution to k_{NR}^{ex} through intersystem crossing is very small as long as the exciplex has $c^2 > 0.2$.

A detailed inspection of Figures (3–5) shows that k_{NR}^{ex} plots generally have lesser slope and curb upward in the CRIP region in comparison to k_f^{ex} plots. It is expected that both types of plots should be nearly parallel since the probabilities of fluorescence and internal conversion (as represented by k_f^{ex} and k_{NR}^{ex}) both derive the amplitude from the corresponding probabilities of *$DBMBF_2$ [e.g., that shown in Equations (3–5)].[13, 14] We suggest that as c^2 and $h\nu_{max}$ of exciplexes shift to the lower (i.e., to more polar) region, the intersystem crossing become more probable *from the increasing contribution of the CT coupling integral* in Equation (6).[13] This emerging new nonradiative process (i.e., ${}^1{*}(AD) \rightarrow {}^3{*}(AD)$, an extra process in Scheme 1) gains importance to boost the k_{NR}^{ex} values as the exciplex CT% increases; k_{NR}^{ex} eventually bottoms-out the decreasing trend in the CRIP region. In effect, we propose that exciplexes, as their polarity increases, are more prone to undergo intersystem crossing, which may become a major contributor to k_{NR}^{ex} in the CRIP region. It implies that in the "inverted" region nonradiative return electron transfer may contain an increasing component of the intersystem crossing channel. In the literature it is known that the rate of intersystem crossing is largely influenced by the extent of spin–orbit coupling, and relatively insensitive to the electronic energy gap (exciplex energy $h\nu_{max}$).[15] Further it has been suggested that spin–orbit coupling is enhanced by CT interactions,[14, 15a] that supports the above proposal. Thus, in the polar region, we have identified the turning point of these plots to shift into the Marcus "inverted region" from the "normal region, and further suggested an increased intersystem crossing as the source feeding the k_{NR}^{ex} upturn.

There is no deep theoretical bases for the plot in Figure 1 in which the quantum yield Φ_{ex}^{∞} and ν_{max} are indirectly related through k_f^{ex} determinations in Equations (2) and (5).[13] Nevertheless, the fact that the fluorescence quantum yield decreases concurrently with the decrease of ν_{max} should hint the presence of an additional nonraditive process in the highly polar exciplexes. The enhanced occurrence of the intersystem crossing and its contribution to k_{NR}^{ex} in the CRIP region as discussed above should be the logical explanation. The extrapolation of the plots of Figure 1 to the highest end at $\nu_{max} = 25 \times 10^3\,cm^{-1}$ ($c^2 = 0.8$) provides the maximum $\Phi_{ex}^{\infty} = 0.6$ of this exciplex system. This drastic Φ_{ex}^{∞} enhancement from *$DBMBF_2$ fluorescence ($\Phi = 0.045$) demonstrates that the emission probability of this exciplex series is primarily derived from the contribution of the LE state in analogy to the reported case.[11, 15] This is the *controlling* force in the Marcus "normal" region, and *differs* from that of return electron transfer[6] in the "inverted" region. This argument implies that the exciplex Φ_{ex}^{∞} can go higher still in a *DBMBF2 interaction with a substrate of higher oxidation potential than benzene ($E_{ox}^{D} = 2.62$ eV). Indeed exciplexes from methyl benzoate and benzonitrile exhibited more intense fluorescence spectra than that shown from benzene; unfortunately, their Φ_{ex}^{∞} could not be measured owing to the superposition of the new fluorescence with the old, and has been approximated[3b] to be > 0.6.

The exciplex decay kinetics should be related to the singlet excited state *$DBMBF_2$ photocycloadditions. In this exciplex series the cycloaddition to benzene and toluene[1b] have been shown to occur with moderate efficiency in competition to much more efficient fluorescence;[3b] the rate constant of the reaction is a part of k_{NR}^{ex} which is substantial at this range. The

  0947-6539/00/0616-2946 $ 17.50+.50/0 *Chem. Eur. J.* **2000**, *6*, No. 16

interaction of *$DBMBF_2$ with olefins does not give exciplex emission, presumably owing to very efficient cycloaddition from the undetected exciplexes.[1a] The reason of inefficient emission and extremely efficient cycloaddition are not clearly understood, but two processes are competitive. It may be mentioned that the efficient quenching distance of *$DBMBF_2$ fluorescence is generally shorter for olefins than for arenes when comparing the members of a same oxidation potential.[3a] This may suggest that olefins generally bind tighter on complex formation with *$DBMBF_2$ and undergo faster cyclization.

Returning now to Figure 2, the bending down from the unit slope in the high E_{ox}^{D} area may originate in a low estimations of c^2, that, in turn, must arise from too high estimation of dipole moment in exciplexes derived from xylenes and lower members. Indeed, in this region, the spectral shape must be distorted owing to overlaps of emission from *DBMBF2 and the relevant exciplexes. Further the spectral overlap necessitate the mathematical partition to give the exciplex spectra, estimation errors of which can be carried over in subsequent calculations to cause deviation by indirect routes.

Conclusion

The series of *$DBMBF_2$ exciplexes derived from the interaction with alkylbenzenes possess the LE state contribution ranging from non-zero to $c^2 = 0.8$ that regulates the transition matrix element to generate the driving force for the exciplex radiative and nonradiative decays in the Marcus "normal" region. This series shows exciplex properties considerably different from CRIP exciplexes wherein the radiative and nonradiative processes are induced by return electron transfer. First of all, Φ_{ex}^{∞} in cyclohexane is drastically enhanced from that of *$DBMBF_2$, and linearly correlated with the fluorescence peak energy ν_{max}. Secondly, k_f^{ex} computed as the function of ν_{max} and c^2 on the basis of exciplex wavefunction gives good agreement with the experimental values. Thirdly, both k_f^{ex} and k_{NR}^{ex} increase with the same trend and as the electronic energy gap for the transitions increases; the better correlation with $h\nu_{max}$ and c^2 rather than with $-\Delta G_{-et}$ demonstrate importance of the stabilization energy U_s arising from the resonance interaction $|A^{-}D^{+}\rangle \rightleftharpoons |{}^{*}AD\rangle$. Thus, in the Marcus "normal" region, the real driving force of exciplex decays is not $-\Delta G_{-et}$ but that modified by U_s.

In Figure 3, k_{NR}^{ex} plots show less steep slopes than k_f^{ex} plots and begin to deviate upward (i.e., the reversal of k_{NR}^{ex} decreases) as CT% increased toward the CRIP region, which is identified as the turning point from the "normal" to "inverted" region. We propose that the k_{NR}^{ex} value is boosted by an emerging contribution of the intersystem crossing process which is induced by exciplex polarity.

Experimental Section

The materials and instruments were the same as those described in the previous papers.[3b, c] The determination of fluorescence spectra, the calculation of the intensity derived from exciplexes and of the quantum yields, solvatochromic shift plots, the calculation of exciplex dipole moments, the determination of exciplex lifetimes were the same as those used in these two papers.

Acknowledgement

The financial supports from Natural Science and Engineering Council of Canada (to Y.L.C.) and the National Science Foundation of China (to Z.L.L.) are gratefully acknowledged. J.I. is grateful for the award of Oversea Research Fellowship from the Japanese Government, Ministry of Education, Science, Sports and Culture. Y.L.C. wishes to thank NLAOC, Lanzhou University for hospitality during the preparation of this manuscript.

[1] a) Y. L. Chow, X.-E. Cheng, *Can. J. Chem.* **1991**, *69*, 1575; b) Y. L. Chow, X. X. Ouyang, *Can. J. Chem.* **1991**, *69*, 423; c) Y. L. Chow, X.-E. Cheng, S. S. Wang, S. P. Wu, *Can. J. Chem.* **1997**, *75*, 720.

[2] a) Y. L. Chow, X.-E. Cheng, *Can. J. Chem.* **1991**, *69*, 1331; b) Y. L. Chow, M. Vanossi, S. S. Wang, *J. Photochem. Photobiol. A: Chem.* **1995**, *88*, 125; c) Y. L. Chow, S. S. Wang, Z. L. Liu, V. Wintgens, P. Valat, J. Kossanyi, *New J. Chem.* **1994**, *18*, 923.

[3] a) Y. L. Chow, S. S. Wang, C. I. Johansson, Z. L. Liu, *J. Am. Chem. Soc.* **1996**, *118*, 11725; b) Y. L. Chow, C. I. Johansson, *J. Phys. Chem.* **1995**, *99*, 17558; c) Y. L. Chow, C. I. Johansson, *J. Phys. Chem.* **1995**, *99*, 17566.

[4] Y. L. Chow, X.-E. Cheng, C. I. Johansson, *J. Photochem. Photobiol. A: Chem.* **1991**, *57*, 247.

[5] a) I. R. Gould, S. Farid, *Acc. Chem. Res.* **1996**, *29*, 522; b) I. R. Gould, R. H. Young, R. E. Moody, S. Farid, *J. Phys. Chem.* **1991**, *95*, 2068; c) I. R. Gould, D. Ege, J. E. Moser, S. Farid, *J. Am. Chem. Soc.* **1990**, *112*, 4290.

[6] a) I. R. Gould, D. Noukakis, J. L. Goodman, R. H. Young, S. Farid, *J. Am. Chem. Soc.* **1993**, *115*, 3830; b) I. R. Gould, D. Noukakis, L. Gomez-Jahn, J. L. Goodman, S. Farid, *J. Am. Chem. Soc.* **1993**, *115*, 4405; c) I. R. Gould, S. Farid, *J. Photochem. Photobiol. A: Chem.* **1992**, *65*, 133.

[7] a) G. Jones III in *Photoinduced Electron Transfer*, *Part A* (Eds.: M. A. Fox, M. Chanone), Elsevier, Amsterdam, **1988**, p. 245; b) N. Mataga, M. Ottolenghi in *Molecular Association*, *Vol. 2* (Ed.: R. Foster), Academica Press, New York, **1979**, p. 1; c) A. Weller in *The Exciplex* (Eds.: M. Gordon, W. R. Ware), Academic, New York, **1975**, p. 23; d) J. Michl, V. Bonacic-Koutecky, *Electronic Aspects of Organic Photochemistry*, Wiley, New York, **1990**, Chapter 5.

[8] N. J. Turro, *Modern Molecular Photochemistry*, Benjamin/Cummings, Menlo Park, CA, USA, **1978**, Chapter 6.

[9] R. S. Mulliken, W. B. Person, *Molecular Complexes*, *A Lecture and Reprint Volume*, Wiley, New York, **1969**.

[10] H. Beens, A. Weller, *Organic Molecular Photophysics*, *Vol. 2* (Ed.: J. B. Birks), Wiley, London, **1975**, Chapter 4.

[11] J. Prochorow, R. Siegoczyñski, *Chem. Phys. Lett.* **1969**, *3*, 635.

[12] T. Shibuya, *J. Chem. Phys.* **1983**, *78*, 5175; T. Shibuya, *Chem. Phys. Lett.* **1983**, *103*, 46.

[13] a) B. T. Lim, S. Okajima, A. K. Chandra, E. C. Lim, *Chem. Phys. Lett.* **1981**, *79*, 22; b) I. Deperasiñska, J. Prochorow, A. Sobolewski, *Chem. Phys.* **1978**, *32*, 257.

[14] H. F. Davis, S. K. Chattopadhyay, P. K. Das, *J. Phys. Chem.* **1984**, *88*, 2798.

[15] a) S. P. McGlynn, T. Azumi, M. Kinoshita, *Molecular Spectroscopy of the Triplet State*, Prentice-Hall, New Jersey, **1969**, p. 284; b) A. R. Watkins, *J. Phys. Chem.* **1979**, *83*, 1892; A. R. Watkins, *Chem. Phys. Lett.* **1976**, *43*, 299.

Received: July 15, 1999
Revised version: March 2, 2000 [F1917]